Electronic structure of a quasi-one-dimensional insulator: The molybdenum red bronze $K_{0.33}MoO_3$

S. Mitrovic, L. Perfetti, C. Søndergaard, G. Margaritondo, and M. Grioni
Institut de Physique des Nanostructures, Ecole Polytechnique Fédérale de Lausanne, CH-1015 Lausanne, Switzerland

N. Barišić and L. Forró
Institut de Physique de la Matière Complexe, Ecole Polytechnique Fédérale de Lausanne, CH-1015 Lausanne, Switzerland

L. Degiorgi
PSI, CH-5232 Villigen, Switzerland
and Laboratorium für Festkörperphysik, ETH Zurich, CH-8093 Zurich, Switzerland

(Received 22 May 2003; revised manuscript received 30 July 2003; published 13 January 2004)

High-resolution angle-resolved photoemission (ARPES) displays quasi-one dimensional (1D) electronic states in the insulating molybdenum red bronze $K_{0.33}MoO_3$, in good qualitative agreement with band structure calculations. Combined ARPES, optical conductivity, and electrical resistivity data underline the importance of defects which pin the Fermi level within the gap. The ARPES line shape exhibits the same strong-coupling features observed in the blue bronze $K_{0.3}MoO_3$, a related 1D Peierls conductor. We speculate that a similar mechanism could be at the origin of the gaps in both materials.

DOI: 10.1103/PhysRevB.69.035102 PACS number(s): 71.45.Lr, 71.10.Pm, 71.38.Cn, 79.60.−i

I. INTRODUCTION

Low-dimensional, and especially quasi-one-dimensional (1D), materials are of current interest because of their unique physical properties and electronic instabilities, which are well documented by structural, thermodynamic, spectroscopic, and transport measurements.[1] Photoemission, in particular, has revealed peculiar aspects of these systems.[2] In 1D conductors, the absence of a clear Fermi edge in momentum-integrated (PES) spectra, and unusually broad angle-resolved (ARPES) line shapes, are clearly incompatible with the spectral properties of normal (2D or 3D) metals.[3–6] Such anomalies could point out strong and singular 1D correlations, and possibly the breakdown of the Fermi liquid paradigm predicted by theory strictly in 1D.[7,8]

Tackling this arduous problem requires broadening the still limited spectroscopic database on 1D materials. Experiments so far mainly addressed 1D conductors, which exhibit characteristic low-energy properties, and low-temperature metal-insulator transitions. Conventional 1D ''band insulators'' were deemed less interesting, but this is not necessarily the case. Some features of optical and ARPES measurements of semiconducting $(NbSe_3)_4I$, namely the unusually small quasiparticle (QP) scattering rate, cannot be explained by prevailing models.[9] 1D band insulators are also useful references for the metallic systems, since the low-energy electron-hole excitations which destroy the QP's and lead to Luttinger liquid (LL), are ''frozen'' by the energy gap. The persistence of peculiar spectral line shapes in the insulators would set new constraints on the interpretation of the electronic properties of 1D materials.

The molybdenum bronzes $A_xMo_yO_z$ (where A is an alkali metal) offer unique opportunities to investigate low-dimensional metallic and insulating systems with closely related structural and electronic properties.[10] The most studied members of this family are the metallic 1D blue bronzes ($x=0.3$), which exhibit Peierls instabilities towards low-temperature charge density wave (CDW) insulating states. Optics[11] and photoemission[12–14] studies of the potassium blue bronze (BB) $K_{0.3}MoO_3$, confirmed various aspects of the weak-coupling Peierls scenario, including the nesting properties of the Fermi surface and the occurrence of pretransitional fluctuations, but also provided evidence for strong electron-phonon interactions.[12] The 1D red bronzes $A_{0.33}MoO_3$ are insulators at all temperatures. The purple bronzes $A_{0.9}Mo_6O_{17}$ are two-dimensional—with ''hidden'' 1D character[15] and nesting[16,17]—and exhibit metal-to-metal CDW instabilities, with the notable exception of the 1D Li purple bronze.

Here we present an ARPES study of the electronic structure of the red bronze (RB) $K_{0.33}MoO_3$, and new optical conductivity and electrical resistivity data. We report a qualitative agreement between the measured 1D dispersion and band structure calculations. We also show that defects states pin the Fermi level in the semiconducting gap. Similarities between the ARPES line shapes of metallic BB and insulating RB suggest that electron-phonon interactions are similarly strong, and may lead to the formation of strongly renormalized polaronic carriers in both materials.

II. STRUCTURAL AND ELECTRONIC PROPERTIES

The Mo red bronze crystallizes in a monoclinic structure (space group $C2/m$), with $\boldsymbol{a}=14.278$ Å, $\boldsymbol{b}=7.723$ Å, $\boldsymbol{c}=6.387$ Å, and $\beta=92.3°$. As for all Mo bronzes, the fundamental structural building blocks are MoO_6 octahedra, which form corner-sharing double chains running along the crystallographic **b** direction (see Fig. 1). The periodicity b along the chain corresponds to two MoO_6 units, due to the presence of lateral—or ''hump''—octahedra. Corner- and edge-sharing double chains are arranged into infinite layers parallel to the c direction, which alternate along the a direction with cation layers.

The structure is essentially two-dimensional, but intra-

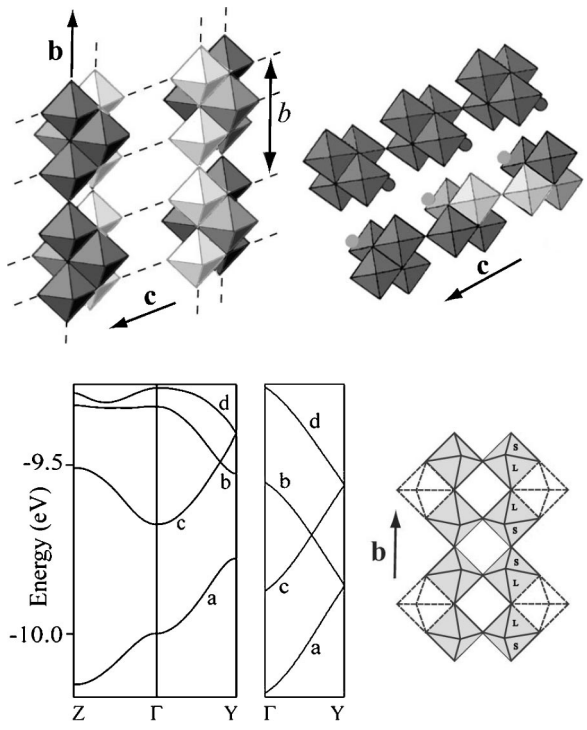

FIG. 1. (Top) left: Double chains of ideally undistorted MoO_6 octahedra run along the **b** axis. One such double-chain (light shade) is shown split for clarity. Right: view along the **b** axis, showing layers of clusters alternating with K layers along the **a** direction. (Bottom) left: The bottom portion of the t_{2g}-block bands, for the real (left) and the hypothetical undistorted structure (right). Right: Schematic view of the symmetry-breaking bond length alternation of short (*S*) and long (*L*) bonds within a real double chain (adapted from Ref. 18).

chain interactions are predominant, and the electronic structure acquires a pronounced 1D character. It can be described considering the overlap of Mo and O orbitals along the chain.[18] The relevant states are Mo $4d(t_{2g})$ and O $2p$ orbitals, which hybridize to form π (bonding) and π^* (antibonding) bands straddling the Fermi level. An ideal undistorted chain would be semimetallic, with a filled valence and an empty conduction band degenerate at the zone boundary Y. In reality, the MoO_6 octahedra are distorted, with an alteration of long-long-short-short Mo-O bonds along the chain. The distortion, which is also periodic with periodicity *b*, lifts the degeneracy, and the red bronze is predicted to be a semiconductor with an indirect gap $\Delta \sim 0.1$ eV (Fig. 1). This is notably different from metallic BB, where a different arrangement of the MoO_6 octahedra leads to two partially filled bands which share the valence electrons.

RB is insulating at all temperatures, and there are no structural indications of CDW instabilities, even if the reported nonlinear transport and a large maximum of the dielectric constant are analogous to CDW-related properties in BB.[19,20] The presence of unusually long (2.069 Å) MoO_6 bonds along the chain has led to the hypothesis of a Coulomb-driven localization of the *d* electrons, and to an alternative interpretation of the energy gap as a correlation (Mott-Hubbard) rather than a band gap.[21] That picture is not supported by band structure calculations which yield similar bandwidths for RB and BB, nor by magnetic susceptibility and ESR data which indicate a very small spin density.[22,23] The present ARPES data provide a direct experimental determination of the valence band in RB, and definitely rule out the Mott-Hubbard scenario.

III. EXPERIMENTAL

Single crystals of RB were grown as described in Ref. 24, in the form of shiny red platelets, less than a millimeter thick, with surfaces of $\sim 3 \times 3$ mm^2 parallel to the crystallographic (100) planes which contain the 1D chains. The crystals, oriented by Laue diffraction, were cleaved in ultrahigh vacuum at a base pressure of 10^{-10} mbar to expose fresh surfaces. We utilized a He discharge lamp ($h\nu = 21.2$ eV) and a Scienta ESCA 300 hemispherical analyzer with energy and momentum resolution $\Delta E = 10$ meV and $\Delta k = 0.04$ Å. The ARPES results were reproduced on various cleaves and different samples. The Fermi level position was determined from the spectrum of a polycrystalline Ag sample, with an accuracy of ± 0.5 meV. We verified that charging did not distort or cause spurious shifts of the spectra by varying the photon intensity.

Electrical resistivity measurements were performed by a standard four-point contact technique between 300 and 800 K. The optical reflectivity was measured on a specimen from the same batch, in the spectral range from the far-infrared up to the ultraviolet for light polarized along and perpendicular to the chain direction, using the equipment described elsewhere.[25] The Kramers-Kronig transformations were then applied in order to obtain the optical functions, namely, the real part $\sigma_1(\omega)$ of the optical conductivity. To this end standard extrapolations, at low and high energies, were employed. Because of the insulating state of RB, the reflectivity was extrapolated to a constant value in the limit of zero frequency.

IV. RESULTS AND DISCUSSION

The longitudinal dc electrical resistivity (Fig. 2) exhibits a semiconducting temperature dependence. Two distinct energy gaps can be identified: $\Delta = 1.36$ eV above ~ 600 K and $\Delta^* = 0.44$ eV below ~ 450 K. No simple activated behavior can be defined at intermediate temperatures. We interpret the larger gap Δ as the full semiconducting gap, and the smaller one as evidence for ''midgap'' states. Their contribution is negligible at high temperatures, but dominates the resistivity at low temperature, where the number of carriers thermally excited across the fundamental gap is small. This assignment is supported by the ARPES data discussed below.

Figure 3 shows $\sigma_1(\omega)$ at 300 K up to the visible spectral range for light polarized along the chain axis. Our optical data agrees with previous results obtained on samples from a different origin.[26] The low-frequency part of the spectrum shows many phonon lines due to the large number of atoms (52) in the primitive unit cell. The analysis of the phonon modes is complex, and beyond the scope of the present paper. We concentrate instead on the high-frequency spectral

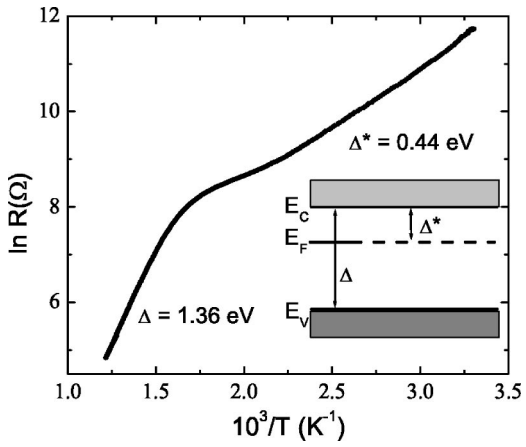

FIG. 2. Temperature dependence of the dc electrical resistance measured along the chain direction. The observation of two distinct gaps (Δ and Δ^*) is consistent with midgap states which pin the Fermi level (inset).

range. The dominant feature is the broad absorption centered at about 8000 cm^{-1} ($\sim$1 eV), which we ascribe to the optical insulating band gap. Another remarkable feature is the shoulder on the low frequency side of the gap at about 5500 cm^{-1} ($\sim$0.68 eV), which again we attribute to ''midgap'' states. The optical gap absorption comes rather close to the square-root singularity expected for a 1D band insulator. On the high-frequency tail of the gap feature, $\sigma_1(\omega)$ approximately decays with an ω^{-3} power law, indicative of a rigid lattice where only umklapp scattering off the single-period lattice potential is possible.[27] This frequency dependence, however, can be verified only over a limited spectral range, due to an overlap with high-energy interband transitions.

The ARPES intensity map of Fig. 4 shows dispersion

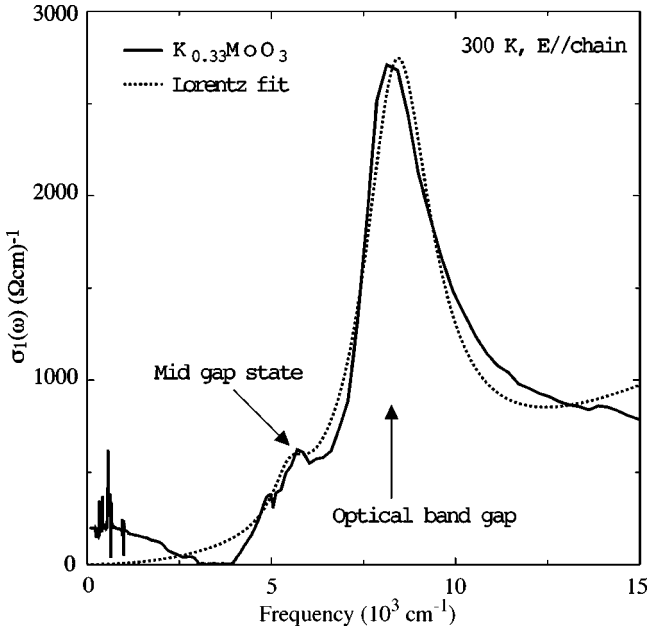

FIG. 3. Real part of the optical conductivity of RB, measured with the light polarized along the chains.

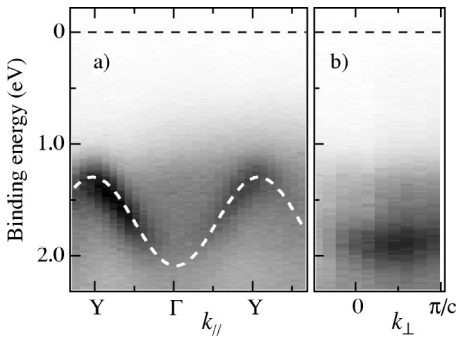

FIG. 4. ARPES intensity maps (a) parallel and (b) perpendicular to the chain direction. The dashed (cosine) line is a guide to the eye.

along the 1D chain direction, with a minimum at Γ ($E_B = 2.1$ eV) and maxima ($E_B = 1.3$ eV) at the zone boundaries $Y(\pm \pi/b)$. At variance with the BB case, there is only one valence band in RB, and its periodicity coincides with the periodicity of the lattice. This band is quite similar to the bonding valence band of BB,[12] but it is rigidly shifted by $\sim$1 eV towards higher binding energies. The narrow-band, Mott insulator scenario of Ref. 21 is not confirmed by the experiment. The measured dispersion $\Delta E = 0.8$ eV is four times larger than the tight binding value. A similar difference in BB was eliminated by subsequent first-principle calculations,[28] and we expect that improved band calculations would be able to reproduce the ARPES dispersion.

Weaker ''shadows'' of the main band extend beyond the zone boundaries into the second Brillouin zone. Shadow bands were also observed in BB and in other 1D Peierls systems such as $(TaSe_4)_2I$ (Ref. 29). While the periodicity of the bands is a ''geometrical'' property, simply reflecting the periodicity of the atomic arrangement, the intensity of the ARPES features, and the gap size, depend on the strength of the periodic—lattice or CDW—potential.[30] In Peierls systems such as $(TaSe_4)_2I$—and possibly also in $(NbSe_4)_3I$—the broad energy gaps and well visible shadows reflect lattice distortions associated with the CDW. The spectral features of Fig. 4 bear clear resemblance to those cases. The hump octahedra (Fig. 1) double the ''geometrical'' periodicity along the chains, defining the size of the Brillouin zone (BZ). They also impose strong constraints on the inner octahedra and induce a deformation of the chain, which provides the necessary periodic potential to open a wide gap.

The experimental gap is considerably larger than the calculated one, but the tight-binding scheme underestimates the Mo d–O p antibonding interactions which remove the degeneracy of the perfect chain.[31] This raises the question of the origin of the distortion. Steric considerations are obviously important, but electronic contributions could also play a role. The periodicity of the distortion coincides with that of a hypothetical Peierls distortion ($2k_F = 2\pi/b$), suggesting the possibility of an instability with a very high critical temperature. This hypothesis would define a common framework for all 1D Mo bronzes, and justify the transport anomalies of RB.[19,20]

The dispersion perpendicular to the chains is extremely small. The map of Fig. 4(b) refers to a line in k-space parallel

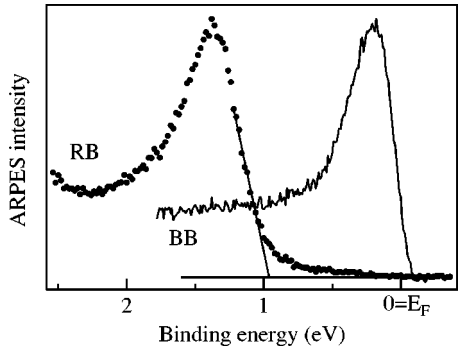

FIG. 5. Comparison of the spectral lineshapes of BB (from Ref. 12) and RB measured, respectively, at the Fermi wave vector and at the top of the valence band.

to the *c* axis, for a fixed wave vector ($k_{\|}=0.4\ \Gamma Y$) along the chains. The dispersion is <0.05 eV, smaller than the calculated value ($\Delta E\sim 0.1$ eV).[18] Therefore, RB appears even more one-dimensional than in the tight binding description. This conclusion should be tested against state-of-the-art first principle calculations, and is moderated by the known surface sensitivity of ARPES. The ARPES dispersion correctly follows the bulk periodicity, but small rearrangements (relaxation) at the surface could influence the overlap of the atomic orbitals, and affect the measured dispersion.

ARPES only probes occupied electronic states, and cannot measure the full gap. A further complication comes from the peculiar 1D line shape. ARPES data on related 1D compounds such as the BB and $(TaSe_4)_2I$, but especially on insulating $(NbSe_4)_3I$, have shown that identifying the peak position with the QP energy would lead to a gross overestimation of the energy gaps. It was found instead that the spectral leading edge is a good indicator of the QP energy both in the metallic and in the insulating phases,[12,29] as a consequence of strong interactions and QP renormalization. We have determined the energy position of the spectral leading edge (Fig. 5) at the top of the band, and obtained E^* ~ 1 eV. This defines the position of the valence band maximum E_V relative to the Fermi energy E_F (Fig. 2, inset). A similar value is obtained from a comparison with the spectrum of BB measured at the Fermi wave vector k_F in the metallic phase, where the QP energy coincides with E_F. Again, an energy shift of ~ 1 eV would be necessary to superimpose the two line shapes.

ARPES and transport data can be reconciled if we assume that impurity (or defect) states, located ~ 0.4 eV below E_C, pin the Fermi level, and define the resistivity gap Δ^* (Fig. 2, inset). They could be associated with oxygen vacancies, or other defects, and are not confined to the surface region probed by ARPES. A very small density of impurities would be sufficient to pin the Fermi energy and determine the low-temperature behavior of the resistivity. The only measurable effect on ARPES would be the observed rigid shift of the valence band by $(\Delta\text{-}\Delta^*)\sim 1$ eV. Such a scenario is also consistent, at least qualitatively, with the optical conductivity (Fig. 3). The quantitative discrepancy between ARPES and optical gaps is not uncommon for 1D materials, e.g., the organic Bechgaard salts.[25] The disagreement between optics

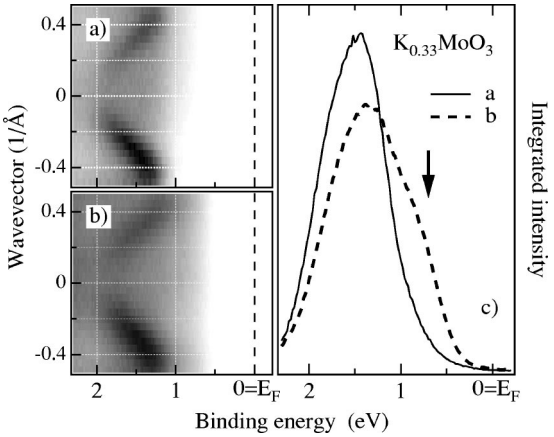

FIG. 6. Comparison of ARPES intensity maps of a ''good cleave'' (a) as in Fig. 4, a ''bad cleave'' (b), and the corresponding momentum-integrated spectra (c).

and transport is more surprising. In 1D systems with broken symmetry ground state, the optical gap (Δ_{opt}) is usually larger than the transport gap (Δ_{tr}) due to the band dispersion perpendicular to the chains, and the discrepancy increases with increasing deviations from perfect nesting[32]. In BB, for instance, $\Delta_{tr}/\Delta_{opt}\sim 0.6$. We do not have a firm explanation for the observation of an optical gap *smaller* than the transport gap in RB. We speculate on a general ground that such differences may be due to different curvatures of the band probed by different experiments. Moreover, only the optical measurements are at the same time bulk sensitive and contactless, and we cannot exclude a possible influence of the interface and of the outermost surface layers both in the transport and ARPES.

We did occasionally observe evidence for surface defects. Such ''bad'' surfaces could not be identified by visual inspection, but their spectra contained spurious features, as shown in Fig. 6. The ARPES map of a ''bad'' cleave [Fig. 6(b)] exhibits the dispersive band of a representative ''good'' surface [Fig. 6(a)], but also diffuse, nondispersive, intensity at lower binding energy. For the ''good'' surface, a momentum-averaged spectrum [Fig. 6(c)] obtained by integrating the intensity map over the whole BZ is consistent with published photoemission data.[33] The spectrum of the ''bad'' surface exhibits a spurious shoulder at ~ 0.6 eV (arrow). Both the ARPES and the integrated data are indicative of defects and inhomogeneous pinning of E_F across the surface. Inhomogeneous pinning and its spectral consequences are well documented effects in semiconductors, a classic example being the (110) surface of GaAs (Ref. 34).

On most surfaces the emission within the gap, and therefore the amount of inhomogeneous pinning was quite small (Fig. 4). This allows us to draw a conclusion which is relevant for all Mo bronzes. Charge balance in these compounds critically depends on the exact K stoichiometry, and it is not guaranteed *a priori* at cleaved surfaces, raising concerns about the ARPES results. A sizable K excess or deficiency at the surface of a semiconductor such as the RB, would have large effects on the spectra, since the Fermi level would be pinned either at E_V or at E_C. On the contrary, we

observe that the Fermi level is always pinned within the gap. Therefore, the stoichiometry of the cleaved surfaces is robust in RB, and we can at least presume that charge neutrality is similarly satisfied at the surfaces of other (metallic) bronzes.

Finally, we briefly consider the spectral ARPES line shape of the RB. Circumstantial evidence for the characteristic spin-charge separation of the LL scenario, has been obtained from data on the 1D bronze $Li_{0.9}Mo_6O_{17}$,[35] and on artificial nanostructures.[36] Alternative interpretations of the data are, however, possible.[37] In particular, in the presence of strong electron-phonon interactions, the resulting spectral weight renormalization could mask the LL features.[29] This might well be the case in Peierls systems such as the blue bronze, where a polaronic (Gaussian) lineshape provides a satisfactory description of the spectra. A comparison of the spectra of Fig. 5 shows that the line shape of the metal and of the insulator are essentially identical, if the Fermi cutoff in the BB spectrum is taken into account. Both line shapes are much too broad ($\Delta E \sim 0.5$ eV) to be interpreted as the spectra of normal QP's. On the other hand, a polaronic scenario[29,38,39] provides a rationale for the unusual width and for the discrepancy between peak and leading edge energies in terms of phonon sidebands, representing the dressing of the heavy (polaronic) QP. This is also supported by optics. A detailed analysis of the optical conductivity indicated a large electron-phonon coupling constant $\lambda \sim 1.2$ in BB,[40] and from a comparison we infer a similarly large coupling in RB. In summary, similarities in the spectral properties of BB and RB ARPES suggest that the dominant factor in both materials is the strong coupling of electrons to the lattice. This, in turn, lends further support to the interpretation of the nature of the static deformation in terms of an electronic instability.

V. CONCLUSIONS

We have determined by ARPES the electronic structure of the quasi-one-dimensional insulator $K_{0.33}MoO_3$ (red bronze). In agreement with band structure calculations, we find a single valence band, with strong 1D character. Its broad bandwidth (~ 1 eV) appears incompatible with an interpretation of the insulating gap in terms of a Mott transition. The spectral properties (dispersion, line shape) of the red bronze are remarkably similar to those of the metallic 1D blue bronze $K_{0.3}MoO_3$, where strong electron-phonon interactions lead to polaronic quasiparticles and to a broken-symmetry (CDW) insulating ground state. A similar mechanism could be invoked to explain the formation of a commensurate distortion and the energy gap in the red bronze. In this perspective, the red bronze could even be a metal at sufficiently high temperatures. This hypothesis would be hard to test experimentally, because the transition would most likely occur outside the range of stability of the compound, but total energy calculations could shed light on this intriguing possibility.

ACKNOWLEDGMENTS

We thank K. Kamaras for the generous loan of the crystals, and acknowledge stimulating discussions with E. Canadell. This work has been supported by the Swiss NSF through the MaNEP NCCR.

[1] G. Grüner, *Density Waves in Solids* (Addison-Wesley, Reading, MA, 1994).

[2] For a recent review see M. Grioni and J. Voit, in *Electron Spectroscopies Applied to Low-Dimensional Materials*, edited by H. P. Hughes and H. I. Starnberg (Kluwer, Dordrecht, 2000), p. 209.

[3] R. Claessen, R.O. Anderson, G.-H. Gweon, J.W. Allen, C.G. Olson, C. Janowitz, W.P. Ellis, Z.-X. Shen, M. Skibowski, K. Friemelt, E. Bucher, S. Hüfner, and V. Eyert, Phys. Rev. B **54**, 2453 (1996).

[4] J.J. Paggel, T. Miller, and T.-C. Chiang, Science **283**, 1709 (1999).

[5] T. Valla, A.V. Fedorov, P.D. Johnson, and S.L. Hulbert, Phys. Rev. Lett. **83**, 2085 (1999).

[6] L. Perfetti, C. Rojas, A. Reginelli, L. Gavioli, H. Berger, G. Margaritondo, M. Grioni, R. Gaal, L. Forró, and F. Rullier-Albenque, Phys. Rev. B **64**, 115102 (2001).

[7] F.D.M. Haldane, J. Phys. C **14**, 2585 (1981).

[8] J. Voit, J. Phys.: Condens. Matter **5**, 8305 (1993).

[9] V. Vescoli, F. Zwick, J. Voit, H. Berger, M. Zacchigna, L. Degiorgi, M. Grioni, and G. Grüner, Phys. Rev. Lett. **84**, 1272 (2000).

[10] C. Schlenker, *Low-Dimensional Electronic Properties of Molybdenum Bronzes and Oxides* (Kluwer, Dordrecht, 1990).

[11] A. Schwartz, M. Dressel, B. Alavi, A. Blank, S. Dubois, G. Grüner, B.P. Gorshunov, A.A. Volkov, G.V. Kozlov, S. Thieme, L. Degiorgi, and F. Levy, Phys. Rev. B **52**, 5643 (1995).

[12] L. Perfetti, S. Mitrovic, G. Margaritondo, M. Grioni, L. Forró, L. Degiorgi, and H. Höchst, Phys. Rev. B **66**, 075107 (2002).

[13] G.-H. Gweon, D. Denlinger, J.W. Allen, R. Claessen, C.G. Olson, H. Höchst, J. Marcus, C. Schlenker, and L.F. Schneemeyer, J. Electron Spectrosc. **117**, 481 (2001).

[14] A.V. Fedorov, S.A. Brazovskii, V.N. Muthukumar, P.D. Johnson, J. Xue, L.-C. Duda, K.E. Smith, W.H. McCarrol, M. Greenblatt, and S.L. Hulbert, J. Phys.: Condens. Matter **12**, L191 (2000).

[15] M.-H. Whangbo, E. Canadell, P. Foury, and J.-P. Pouget, Science **252**, 96 (1991).

[16] G.H. Gweon, J.W. Allen, J.A. Clack, Y.X. Zhang, D.M. Poirier, P.J. Benning, C.G. Olson, J. Marcus, and C. Schlenker, Phys. Rev. B **55**, 13353 (1997).

[17] K. Breuer, C. Stagarescu, K.E. Smith, M. Greenblatt, and K. Ramanujachary, Phys. Rev. Lett. **76**, 3172 (1996).

[18] M.-H. Whangbo, M. Evain, E. Canadell, and M. Ganne, Inorg. Chem. **28**, 267 (1989).

[19] B. Zawilski, J. Richard, and J. Marcus, Solid State Commun. **109**, 41 (1999).

[20] B. Zawilski, T. Klein, and J. Marcus, Solid State Commun. **124**, 39 (2002).

[21] G. Travaglini and P. Wachter, Solid State Commun. **47**, 217 (1983).

[22] R. Xiong, J. Shi, Q. Xiao, W. Tang, H. Liu, and D. Tian, J. Mater. Sci. **36**, 5511 (2001).
[23] G.H. Bouchard, J. Perlstein, and M.J. Sienko, Inorg. Chem. **9**, 1682 (1967).
[24] A. Wold, W. Kunnmann, R.J. Arnott, and A. Ferretti, Inorg. Chem. **4**, 545 (1964).
[25] V. Vescoli, F. Zwick, W. Henderson, L. Degiorgi, M. Grioni, G. Gruner, and L.K. Montgomery, Eur. Phys. J. B **13**, 503 (2000).
[26] G. Travaglini, P. Wachter, J. Marcus, and C. Schlenker, Solid State Commun. **42**, 407 (1982).
[27] P.A. Lee, T.M. Rice, and P.W. Anderson, Solid State Commun. **14**, 407 (1974).
[28] J.-L. Mozos, P. Ordejón, and E. Canadell, Phys. Rev. B **65**, 233105 (2002).
[29] L. Perfetti, H. Berger, A. Reginelli, L. Degiorgi, H. Höchst, J. Voit, G. Margaritondo, and M. Grioni, Phys. Rev. Lett. **87**, 216404 (2001).
[30] J. Voit, L. Perfetti, F. Zwick, H. Berger, G. Margaritondo, G. Grüner, H. Höchst, and M. Grioni, Science **290**, 501 (2000).
[31] E. Canadell (private communication).
[32] G. Mihaly, A. Virosztek, and G. Grüner, Phys. Rev. B **65**, 233105 (2002).
[33] K. Terashima, H. Matsuoka, K. Soda, S. Suga, R. Yamamoto, and M. Doyama, J. Phys. Soc. Jpn. **57**, 2557 (1988).
[34] M. Grioni, J.J. Joyce, and J.H. Weaver, Phys. Rev. B **32**, 962 (1985).
[35] J.D. Denlinger, G.-H. Gweon, J.W. Allen, C.G. Olson, J. Marcus, C. Schlenker, and L.-S. Hsu, Phys. Rev. Lett. **82**, 2540 (1999).
[36] P. Segovia, D. Purdie, M. Hengsberger, and Y. Baer, Nature (London) **402**, 504 (1999).
[37] F.J. Himpsel, K.N. Altmann, J.N. Crain, A. Kirakosian, J.-L. Lin, A. Liebsch, and V.P. Zhukov, J. Electron Spectrosc. **126**, 89 (2002).
[38] D.S. Dessau, T. Saitoh, C.H. Park, Z.-X. Shen, P. Vilella, N. Hamada, Y. Moritomo, and Y. Tokura, Phys. Rev. Lett. **81**, 192 (1998).
[39] V. Perebeinos and P.B. Allen, Phys. Rev. Lett. **85**, 5178 (2000).
[40] L. Degiorgi, St. Thieme, B. Alavi, G. Grüner, R.H. McKenzie, K. Kim, and F. Levy, Phys. Rev. B **52**, 5603 (1995).